The Vlasov-Poisson Equations as the Semiclassical Limit of the Schrödinger-Poisson Equations: A Numerical Study*

Shi Jin†, Xiaomei Liao‡and Xu Yang§

October 6, 2008

Abstract

In this paper, we numerically study the semiclassical limit of the Schrödinger-Poisson equations as a selection principle for the weak solution of the Vlasov-Poisson in one space dimension. Our numerical results show that this limit gives the weak solution that agrees with the zero diffusion limit of the Fokker-Planck equation. We also numerically justify the multivalued solution given by a moment system of the Vlasov-Poisson equations as the semiclassical limit of the Schrödinger-Poisson equations.

1 Introduction

We are interested in establishing a selection principle for the weak solution of the following one-dimensional Vlasov-Poisson equations:

$$\frac{\partial f}{\partial t} + v\frac{\partial f}{\partial x} - E(x,t)\frac{\partial f}{\partial v} = 0, \tag{1.1}$$

$$\frac{\partial^2}{\partial x^2}V = \rho = b(x) - \int_{-\infty}^{\infty} f(x,v,t)dv, \quad E = \frac{\partial V}{\partial x}, \tag{1.2}$$

subject to the initial condition

$$f(x,v,t)|_{t=0} = f_0(x,v) \geq 0. \tag{1.3}$$

*Research supported by NSF grant Nos. DMS-0305080 and DMS-0608720.

†Department of Mathematics, University of Wisconsin, Madison, WI 53706, USA. Email: jin@math.wisc.edu

‡Department of Mathematics, University of Wisconsin, Madison, WI 53706, USA. Current address: Department of Biostatistics, Harvard University, Boston, MA, 02115, USA. Email: xliao@hsph.harvard.edu

§Department of Mathematics, University of Wisconsin, Madison, WI 53706, USA. Email: xyang@math.wisc.edu.

In (1.1)-(1.2), $f(x,v,t)$ is the density of electrons at location x traveling with velocity v at time t, ρ is the charge density, $b(x) \geq 0$ denotes the fixed positively charged background, $E(x,t)$ is the electric field and $V(x,t)$ is the electric potential. For simplicity in exposition, we assume throughout this paper that $b(x) = 1$ and $f(x,v,t)$ is 1-periodic in x, i.e.

$$\begin{aligned} &f(x+1,v,t) = f(x,v,t), \quad E(x+1,t) = E(x,t) \\ &\int_0^1 E(x,t)dx = 0. \end{aligned} \tag{1.4}$$

In (1.3), $f_0(x,v)$ is a non-negative probability measure, i.e.

$$\int_0^1 \int_{-\infty}^{\infty} f_0(x,v)dxdv = 1.$$

We first state the definition of a weak solution according to [14].

Definition 1.1. A pair $\{E, f\}$ of a function $E(x,t)$ and a non-negative measure $f(x,v,t)$ is called a weak solution to the problem (1.1)-(1.4), if $\{E,f\}$ is 1-periodic in x and for some $T > 0$,

1. $E \in L^\infty(\Omega_T) \cap BV(\Omega_T)$ where $\Omega_T = [0,1] \times (0,T)$;
2. $f(x,v,t)$ is a probability measure for each $t > 0$,
$$\int_0^1 \int_{-\infty}^{\infty} f(x,v,t)dvdx = 1;$$
3. for all $\phi \in C_0^\infty(\mathbf{R}^2 \times (0,T))$, the velocity average of $f(x,v,t)$ with ϕ is a special measure, which is the x-derivative a BV function $h_\phi(x,t) \in BV(\Omega_T)$, i.e. $\int_{-\infty}^{\infty} \phi(x,v,t)f(x,v,t)dv = \partial_x h_\phi$;
4. $\{E,f\}$ satisfies the Poisson equation in the distributional sense, $E_x = 1 - \int_{-\infty}^{\infty} f dv$, and the normalizing condition is compatible with Condition 2, $\int_0^1 E dx = 0$;
5. $\{E,f\}$ satisfies the Vlasov equation in the weak form:
$$\int_0^T \int_{\mathbf{R}^2} (\phi_t f + \phi_x v f)dvdxdt - \int_0^T \int_{\mathbf{R}} \bar{E} \left(\int_{\mathbf{R}} \phi_v f dv \right) dxdt = 0, \tag{1.5}$$
for all test functions $\phi \in C_0^\infty(\mathbf{R}^2 \times (0,T))$, and $\bar{E}$ is given by
$$\bar{E} = \begin{cases} E(x,t), & \text{if } E \text{ is approximately continuous at } (x,t), \\ \frac{1}{2}[E_l(x,t) + E_r(x,t)], & \text{if } E \text{ has a jump at } (x,t), \end{cases} \tag{1.6}$$
where $E_l(x,t)$ and $E_r(x,t)$ denote respectively the left and right limits of $E(x,t)$ at a discontinuity point.

6. f is Lipschitz continuous from $[0,T]$ to the local negative Sobolev space $H^{-L}_{loc}(\mathbf{R}^2)$ for some $L>0$, and $f(x,v,0)=f_0(x,v)$ in $H^{-L}_{loc}(\mathbf{R}^2)$.

As a regularization to the Vlasov-Poission equation, consider the Fokker-Planck equation satisfies

$$\frac{\partial f^\eta}{\partial t}+v\frac{\partial f^\eta}{\partial x}-E^\eta(x,t)\frac{\partial f^\eta}{\partial v}=\eta\frac{\partial^2 f^\eta}{\partial v^2}, \tag{1.7}$$

$$\frac{\partial^2}{\partial x^2}V^\eta=\rho^\eta=b(x)-\int_{-\infty}^{\infty}f^\eta(x,v,t)dv,\quad E^\eta=\frac{\partial V^\eta}{\partial x}, \tag{1.8}$$

where $\eta\geq 0$ is the viscous coefficient and the initial condition is

$$f^\eta(x,v,t)|_{t=0}=f_0(x,v)\geq 0. \tag{1.9}$$

The existence of suitable weak solutions to (1.1)-(1.3) was established by Zheng and A. Majda ([18]). Moreover, the non-uniqueness issue of (1.1)-(1.3) was discussed by A. Majda, G. Majda and Zheng in [14], where two explicit weak solutions with the same charge concentration initial data were constructed. It was shown that the zero smoothing limit of the time reversible particle method converges to the discrete fission weak solution while the zero diffusion limit of the Fokker-Planck equation (1.7)-(1.8) converges to the continuous fission weak solution.

In this paper, we consider another regularization process given by the semi-classical limit of Schrödinger-Poisson equations, and hope to establish a selection principle for the weak solution of the Vlasov-Poisson equations. The convergence of the limit was studied in [8, 11, 13, 17]. For convenience, we summarize the main results of [17] as below.

The Schrödinger-Poisson equations are

$$\left\{\begin{array}{rcl} i\epsilon\psi^\epsilon_t &=& -\frac{\epsilon^2}{2}\psi^\epsilon_{xx}+V^\epsilon(x)\psi^\epsilon,\\ \partial_{xx}V^\epsilon &=& 1-|\psi^\epsilon(x,t)|^2,\ \ E^\epsilon=\frac{\partial V^\epsilon}{\partial x},\quad x\in\mathbf{R},\ \ t\geq 0,\end{array}\right. \tag{1.10}$$

with the initial condition

$$\psi^\epsilon|_{t=0}=\psi^\epsilon_0. \tag{1.11}$$

Definition 1.2. The Wigner transform of ψ^ϵ is defined as ([16])

$$W^\epsilon(x,v,t)=\frac{1}{2\pi}\int_{\mathbf{R}}e^{-ivy}\psi^\epsilon(x+\frac{\epsilon y}{2},t)\overline{\psi^\epsilon}(x-\frac{\epsilon y}{2},t)dy \tag{1.12}$$

Theorem 1.3. *Let $\varphi_\epsilon(x)$ be uniformly bounded in $L^2(\mathbf{R})$, $b(x)\in(L^1\cap L^2)(\mathbf{R})$, $\psi^\epsilon_0=J_\epsilon*\varphi_\epsilon(x)$, $b^\epsilon=b*J_\epsilon(x)$ where the Friedrichs mollifier $J_\epsilon(x)=\frac{1}{\epsilon}J(\frac{x}{\epsilon})$ and $J(x)=\frac{1}{\pi}e^{-x^2}$. Let $W^\epsilon(x,v,t)$ be the Wigner transform of a solution ψ^ϵ defined in (1.12). Then there is a subsequence of $\{W^\epsilon(x,v,t)\}$, which we still denote by $\{W^\epsilon(x,v,t)\}$ for convenience, and a nonnegative bounded Radon measure $f(x,v,t)$ such that $W^\epsilon(x,v,t)\rightharpoonup f(x,v,t)$ as $\epsilon\to 0$, where the Wigner measure $f(x,v,t)$ is a weak solution of (1.1)-(1.3) in the*

sense of Definition 1.1, with f_0 the Wigner measure of $\psi_0^\epsilon(x)$ and an $L > 2$ in Condition 6 of Definition 1.1. Here, the test function space for the weak convergence is defined as

$$\mathcal{A} = \left\{\phi \in C_c^\infty(\mathbf{R}_x \times \mathbf{R}_v) : (\mathcal{F}_v\phi)(x,\xi) \in L^1(\mathbf{R}_\eta, C_c(\mathbf{R}_x))\right\}$$

with the norm

$$\|\phi(x,v)\|_{\mathcal{A}} = \int_{\mathbf{R}} sup_x \left|(\mathcal{F}_v\phi)(x,\xi)\right| d\xi,$$

where $(\mathcal{F}_v\phi)(x,\xi)$ is the Fourier transformation of $\phi(x,v)$ with respect to v.

Remark 1.4. The same conclusion of Theorem 1.3 still holds if one considers the x-domain to be $[0,1]$ and all the functions are 1-periodic in x, which will allow $b(x) = 1$.

We are interested in which weak solution the semiclassical limit selects for the weak solution of the Vlasov-Poisson equations. Our numerical experiments show that it selects the one obtained by the zero diffusion limit of the Fokker-Planck equations. In addition, we will also check if this limit is sensitive to the numerical regularization of the measure-valued initial data. Our numerical results show that it is not.

We are also interested in the justification of the moment system for the multivalued solutions of the Euler-Poission equations as the correct semiclassical limit of the Schrödinger-Poission equations. It is known that the solution to the Vlasov-Poisson equations with mono-kinetic initial data, like the Liouville or Vlasov equation [9, 15], when projected into the physical space, may become multivalued which cannot be captured by the viscous solution of the single-valued closure–the Euler-Poission equations. A moment system following the work of [9] was introduced in [10] for such multivalued solutions. Multivalued solutions to the Vlasov-Poission equations were also studied later in [7, 12]. So far little rigorous study on the multi-valued solution to the Euler-Poisson equations is available, nor has there been any theoretical or even numerical justification of these multilvalued solutions as the correct semiclassical limit of the Schrödinger-Poission equations. Our numerical results in this paper suggest that the solutions to the moment equations introduced in [10] is the semiclassical limit of the Schrödinger-Poission equations.

The paper is organized as follows. The numerical schemes to solve the Vlasov-Poisson equations, Fokker-Planck equations, and the Schrödinger-Poisson equations are introduced in Section 2. The moment method and its discretization by a kinetic scheme for the multi-valued solution of the Euler-Poission equations is briefly reviewed in Section 3. Four numerical examples are given in Section 4 to justify our conclusion. In Section 5, we give some concluding remarks.

2 Numerical schemes for three types of equations

2.1 A particle method for the 1D Vlasov-Poisson and Fokker-Planck equations

A particle method for the Vlasov-Poisson equations (1.1)-(1.3) was first introduced in [4]. Here we use the slightly modified version in [14] which is summarized below.

The particle trajectory equations are

$$\begin{cases} \frac{dx_j}{dt} = v_j \\ \frac{dv_j}{dt} = -\tilde{E}(x_j, t) \end{cases} \qquad j = 1, \cdots, N, \tag{2.1}$$

with the given initial condition $(x_j(0), v_j(0)) = (x_j^0, v_j^0)$, where x_j is the position of j-th particle, v_j is the velocity of j-th particle, N is the total number of particles.

In (2.1), the approximate electric field is

$$\tilde{E}(x,t) = C\Sigma_{j=1}^{N^*} K_\delta(x, x_j^*) - \Sigma_{j=1}^{N} \alpha_j K_\delta(x, x_j(t)), \tag{2.2}$$

where the points $x_j^* = (j-1)h$ with $h = 1/N^*,\ j = 1, \cdots, N^*$, are uniformly spaced in $[0,1]$. The weights $\alpha_j,\ j = 1, \cdots, N$, are determined by the initial data, and $C = \Sigma_{j=1}^{N} \alpha_j / N^*$ is a constant chosen so that the constrain (1.4) is always satisfied. The modified kernel K_δ is given by

$$K_\delta(x,y) = \begin{cases} y, & y - x \le -\frac{1}{2}\delta, \\ y - \frac{1}{2} - (y-x)/\delta, & -\frac{1}{2}\delta \le y - x \le \frac{1}{2}\delta, \\ y - 1, & \frac{1}{2}\delta \le y - x. \end{cases} \tag{2.3}$$

We approximate the Fokker-Planck equation (1.7)-(1.9) by a random particle method which combines a first-order splitting procedure with a random walk solution of the diffusion equation contained in (1.7). In the time interval $[t, t+\Delta t]$, where $\Delta t > 0$ is some constant, the phase space trajectories are solutions of the approximate particle trajectory equations (2.1) and (2.2) with the initial condition given by

$$(\tilde{x}_j(t), \tilde{v}_j(t)) = (x_j(t), v_j(t) + G_j(0, 2\eta\Delta t)), \tag{2.4}$$

where $G_j(0, 2\eta\Delta t)$ is a Gaussian random variable with mean 0 and variance $2\eta\Delta t$.

2.2 The Time-splitting spectral method for the Schrödinger-Poisson equations

To solve the Schrödinger-Poisson system (1.10)-(1.11), we use the time-splitting spectral method (SP1, [2]). Namely, the Schrödinger equation is solved in two steps. One solves

$$i\epsilon\psi_t^\epsilon + \frac{\epsilon^2}{2}\psi_{xx}^\epsilon = 0 \tag{2.5}$$

for one time step, followed by solving

$$i\epsilon\psi_t^\epsilon - V^\epsilon(x)\psi^\epsilon = 0 \tag{2.6}$$

again for one time step. Eq.(2.5) will be discretized in space by the spectral method and integrated in time exactly. The ODE (2.6) will then be solved exactly. Note that if one uses the Strang splitting method (SP2), i.e. solves (2.5) within half a time step,

(2.6) within one time step, followed by (2.5) within half a time step, then the numerical accuracy in time will be second order.

For Poisson equation $\partial_{xx}V^\epsilon = 1 - \rho^\epsilon$, we also use spectral method. Using the fourier transform, we can get $\hat{V^\epsilon}_k(t) = (\frac{L}{2\pi k})^2(\widehat{1-\rho^\epsilon})_k(t)$, where L is the length of computational domain. And we set $\hat{V^\epsilon}_0(t) = 0$ for every time step. Inverse fourier transform follows after updating $(\widehat{1-\rho^\epsilon})_k(t)$ and $\hat{V^\epsilon}_k(t)$.

3 The moment method for multivalued solutions

Consider the Schrödinger-Poisson equations (1.10) with the WKB initial data

$$\psi_0^\epsilon = A_0(x)\exp(i\frac{S_0(x)}{\epsilon}). \tag{3.1}$$

It was proved in [13, 11, 8, 17] that the weak limit of this initial value problem is the Vlasov-Poisson equations (1.1)-(1.2) with the mono-kinetic initial data

$$f_0(x,v) = |A_0|^2\,\delta(v - \nabla_x S_0). \tag{3.2}$$

If one assumes the mono-kinetic ansatz $f(x,v,t) = \rho(x,t)\delta(v-u(x,t))$ with $\rho(x,0) = |A_0|^2$, $u(x,0) = \nabla_x S_0$, then one can close the Vlasov-Poisson equations (1.1)-(1.2) by the Euler-Poisson system

$$\left\{\begin{array}{rcl} \frac{\partial}{\partial t}\rho + \frac{\partial}{\partial x}(\rho u) &=& 0, \\ \frac{\partial}{\partial t}(\rho u) + \frac{\partial}{\partial x}(\rho u^2) &=& -\rho\partial_x V, \\ \partial_{xx}V &=& 1-\rho. \end{array}\right. \tag{3.3}$$

This is a weakly hyperbolic system. Even if $\rho(x,0)$ and $u(x,0)$ are smooth, singularities (shocks, which corresponds to caustics in geometric optics) form in finite time. Beyond the singularity time, multivalued solution should be introduced. In [9], a moment system was introduced for the Vlasov equation with initial data (3.2). This idea was extended to the Vlasov-Poisson equations in [10].

3.1 The moment system for multi-valued solutions

In this section, we review the moment system, given in [9, 10], for multivalued solutions. First define the moments of the Vlasov-Poisson equations (1.1)-(1.2):

$$m_l = \int_R f(x,v,t)v^l\,dv, \quad l = 0,1,\cdots,2K. \tag{3.4}$$

Then taking moments of (1.1), one can get the moment equations in the physical space

$$\left\{\begin{array}{rcl} \frac{\partial}{\partial t}m_0 + \frac{\partial}{\partial x}m_1 &=& 0, \\ \frac{\partial}{\partial t}m_1 + \frac{\partial}{\partial x}m_2 &=& -m_0\partial_x V, \\ \cdots\ \cdots & & \\ \frac{\partial}{\partial t}m_{2K-1} + \frac{\partial}{\partial x}m_{2K} &=& -(2K-1)m_{2K-2}\partial_x V, \\ \partial_{xx}V &=& 1 - \sum_{k=1}^K \rho_k\,. \end{array}\right. \tag{3.5}$$

Suppose the total number of branches is $K < \infty$, then the solution of (1.1)-(1.2) can be expressed as

$$f(x,v,t) = \Sigma_{k=1}^{K} \rho_k \delta(v - u_k), \tag{3.6}$$

where (ρ_k, u_k) is the density and the velocity for the kth-branch. Then one can express the moments in terms of $(\rho_k, u_k), k = 1, 2, \cdots, K$:

$$m_l = \sum_{k=1}^{K} \rho_k u_k^l, \quad l = 0, 1, \cdots, 2K.$$

m_0 is called the average density, and the average velocity is defined as

$$\bar{u} = m_1/m_0 \tag{3.7}$$

With (3.6), (3.5) can be closed by expressing m_{2K} as a function of $m_0, \cdots, m_{2K-1}$ provided the mapping from $\{(\rho_k, u_k), k = 1, \cdots, K\}$ to $(m_0, m_1, \cdots, m_{2K-1})$ is invertible, thus closing the moment system (3.5).

For the examples we will present later, the value of K is at most 3. We first define the phase indicating functions

$$\begin{array}{rcl} \theta_1 &=& m_0 m_2 - m_1^2 \\ \theta_2 &=& m_4 m_1^2 - m_4 m_2 m_0 + m_3^2 m_0 - 2 m_1 m_2 m_3 + m_2^3 \end{array} \tag{3.8}$$

When $K = 3$, define

$$\begin{array}{rcl} p_1 &=& u_1 + u_2 + u_3 \\ &=& (m_5 m_1^2 - m_5 m_2 m_0 + m_4 m_3 m_0 - m_4 m_1 m_2 + m_3 m_2^2 - m_1 m_3^2)/\theta_2 \\ p_2 &=& u_1 u_2 + u_1 u_3 + u_2 u_3 \\ &=& -(m_5 m_3 m_0 - m_5 m_2 m_1 + m_4 m_2^2 - m_4^2 m_0 + m_4 m_3 m_1 - m_2 m_3^2)/\theta_2 \\ p_3 &=& u_1 u_2 u_3 \\ &=& -(m_5 m_3 m_1 - m_5 m_2^2 - m_4^2 m_1 + 2 m_4 m_3 m_2 - m_3^3 - m_4^2 m_1)/\theta_2 \end{array}$$

Then m_6 can be expressed as $m_6 = m_5 p_1 - m_4 p_2 + m_3 p_3$. So the first six equations of (3.5) are closed.

When $K = 2$, define

$$\begin{array}{rcl} p_1 = u_1 + u_2 &=& (m_3 m_0 - m_1 m_2)/\theta_1 \\ p_2 = u_1 u_2 &=& (m_1 m_3 - m_2^2)/\theta_1 \end{array}$$

Then m_4 can be expressed as $m_4 = m_3 p_1 - m_2 p_2$ and the first four equations of (3.5) are closed.

When $K = 1$, the first two equations of (3.5) are reduced to the Euler-Poisson system (3.3).

The number of phases at the point (x, t) can be identified using the phase indicating functions via

$$\text{Number of phases} = \begin{cases} 1, & if \quad \theta_1 = 0, \\ 2, & if \quad \theta_1 > 0, \theta_2 = 0, \\ 3, & if \quad \theta_2 < 0. \end{cases}$$

3.2 A kinetic scheme for the multi-phase moment system

The second order kinetic scheme is used for the multi-phase system (3.5) (see [9]).

Suppose the computational domain of x is $[a,b]$. Let the mesh size of x be Δx with $\Delta x = (b-a)/M$, and the time step be Δt, then

$$x_j := a + j\Delta x, \quad t_n := n\Delta t, \quad j = 0, 1, \cdots, M, \quad n = 0, 1, 2, \cdots.$$

Multiplying (1.1) with v^l and integrating it over $(x_{j-\frac{1}{2}}, x_{j+\frac{1}{2}}) \times R_v \times (t_n, t_{n+1})$, one gets

$$(m_l)_j^{n+1} - (m_l)_j^n + \frac{\Delta t}{\Delta x}(f_{j+\frac{1}{2}}^{(l+1)} - f_{j-\frac{1}{2}}^{(l+1)}) = -l \cdot (\frac{m_{l-1}^n + m_{l-1}^{n+1}}{2} E^n)_j \cdot \Delta t$$

where

$$(m_l)_j^n = \frac{1}{\Delta x} \int_{x_{j-\frac{1}{2}}}^{x_{j+\frac{1}{2}}} m_l^n \, dx,$$

and

$$f_{j+\frac{1}{2}}^{(l)} = \frac{1}{\Delta t} \int_R \int_{t_n}^{t_{n+1}} f(x_{j+\frac{1}{2}} - vt, v, t) v^l \, dt \, dv.$$

We can use piecewise linear construction for (ρ_k, u_k) to obtain a second order scheme,

$$\begin{cases} \rho(x) &= (\rho)_j + D\rho_j(x - x_j), \\ u(x) &= \bar{u}_j + Du_j(x - x_j), \end{cases} \quad for \quad x_{j-1/2} < x < x_{j+1/2},$$

where $\bar{u}_j$ is chosen as

$$\bar{u}_j = u_j - \frac{D\rho_j Du_j}{12\rho_j} \Delta x^2.$$

With $f(x,v,t) = \sum_{k=1}^K \rho_k \delta(v - u_k)$, then

$$f_{j+\frac{1}{2}}^{(l)} = \sum_{k=1}^K \frac{1}{\Delta t} \int_{x_{j+\frac{1}{2}}^L}^{x_{j+\frac{1}{2}}} \rho_k(x) u_k(x)^{l-1} \, dx - \frac{1}{\Delta t} \int_{x_{j+\frac{1}{2}}}^{x_{j+\frac{1}{2}}^R} \rho_k(x) u_k(x)^{l-1} \, dx,$$

where

$$x_{j+1/2}^L = x_{j+1/2} - \Delta t \frac{(\bar{u}_j + \frac{\Delta x}{2} Du_j)^+}{1 + \Delta t Du_j},$$

and

$$x_{j+1/2}^R = x_{j+1/2} + \Delta t \frac{(u_{j+1/2}^R)^-}{1 + \Delta t Du_{j+1}}.$$

In more explicit forms, we have

$$\begin{aligned} f_{j+\frac{1}{2}}^{(l)} &= \sum_{k=1}^K \sum_{s=0}^{l-1} C_{l-1}^s (\bar{u}_k)_j^s (Du_k)_j^{l-s-1} \Big[\frac{1}{(l-s)\Delta t} (\rho_k)_j \big((\frac{1}{2}\Delta x)^{l-s} - (x_{j+\frac{1}{2}}^L - x_j)^{l-s} \big) \\ &+ \frac{1}{(l-s+1)\Delta t} (D\rho_k)_j \big((\frac{1}{2}\Delta x)^{l-s+1} - (x_{j+\frac{1}{2}}^L - x_j)^{l-s+1} \big) \Big] \\ &- \sum_{k=1}^K \sum_{s=0}^{l-1} C_{l-1}^s (\bar{u}_k)_{j+1}^s (Du_k)_{j+1}^{l-s-1} \Big[\frac{1}{(l-s)\Delta t} (\rho_k)_{j+1} \big((x_{j+\frac{1}{2}}^R - x_{j+1})^{l-s} - (-\frac{1}{2}\Delta x)^{l-s} \big) \\ &+ \frac{1}{(l-s+1)\Delta t} (D\rho_k)_{j+1} \big((x_{j+\frac{1}{2}}^R - x_{j+1})^{l-s+1} - (-\frac{1}{2}\Delta x)^{l-s+1} \big) \Big] \end{aligned}$$

where we choose the slope limiters in the following way ,

$$
\begin{aligned}
D\rho_j &= \frac{1}{2}\Big(\operatorname{sgn}(\rho_{j+1}-\rho_j)+\operatorname{sgn}(\rho_j-\rho_{j-1})\Big)\\
&\quad\times\min\left\{\frac{|\rho_{j+1}-\rho_j|}{\Delta x},\frac{|\rho_j-\rho_{j-1}|}{\Delta x},\frac{2\rho_j}{\Delta x}\right\},\\
Du_j &= \frac{1}{2}\Big(\operatorname{sgn}(u_{j+1}-u_j)+\operatorname{sgn}(u_j-u_{j-1})\Big)\\
&\quad\times\min\left\{\frac{|u_{j+1}-u_j|}{(1-\Delta x D\rho_j/6\rho_j)\Delta x},\frac{|u_j-u_{j-1}|}{(1+\Delta x D\rho_j/6\rho_j)\Delta x},\frac{1}{\Delta t}\right\}.
\end{aligned}
$$

The Poisson equation in (3.5) will be solved by the second order finite difference method.

Let V_j^n, $\rho_{j,k}^n$, E_j^n be the approximation of $V(x_j,t_n)$, $\rho_k(x_j,t_n)$, $E(x_j,t_n)$ respectively, then the discretization of $\partial_{xx}V = 1-\sum_{k=1}^K \rho_k$ is as follows :

$$
\frac{V_{j+1}^n-2V_j^n+V_{j-1}^n}{\Delta x^2} = 1-\sum_{k=1}^K \rho_{j,k}^n \quad\text{and}\quad E_j^n = \frac{V_{j+1}^n-V_{j-1}^n}{2\Delta x}.
$$

4 Numerical examples

Example 4.1. Solve the Schrödinger-Poisson equations (1.10) with the initial condition (3.1) using the SP2 method where $A_0(x)$ is the square root of a δ-function approximated by the cosine kernel (for a recent work on numerical discretization of the delta-function, see [5]):

$$
\psi_0^\epsilon = \sqrt{\delta_b^c(x)}\exp(\frac{iC}{\epsilon}),\quad \text{where } \delta_b^c(x) = \begin{cases} \frac{1}{2b}(1+\cos\frac{|\pi(x-0.5)|}{b}), & \left|\frac{x-0.5}{b}\right|\le 1,\\ 0, & \text{otherwise,}\end{cases} \tag{4.1}
$$

in which C is a constant, and $b = O(\sqrt{\epsilon})$. In numerical implementation, we take $\Delta x = b^2 = O(\epsilon)$, which satisfies the mesh size restriction of SP1 (SP2) methods ([2]).

We solve the Vlasov-Poisson equations (1.1)-(1.2) and the Fokker-Planck equations (1.7)-(1.8) by the particle methods with the measure initial condition $f_0(x,v) = \delta(x-0.5)\delta(v)$.

The Wigner measure of ψ_0^ϵ as $\epsilon\to 0$ is $f_0(x,v) = \delta(x-0.5)\delta(v)$ which allows two weak solutions given by the zero smoothing limit of the time reversible particle methods and the zero diffusion limit of the Fokker-Planck equations respectively ([14]). Since ψ_0^ϵ is uniformly bounded in $L^2(\mathbf{R})$ (the upper bound is 1), Theorem 1.3 implies that the weak limit of a subsequence of $W^\epsilon(t,x,\xi)$, the Wigner transform of the solution of the Schrödinger-Poisson equations with initial condition ψ_0^ϵ, should converge to a weak solution of the Vlasov-Poisson equations.

In Figure 1, one can see that the semiclassical limit solution agrees with the weak solution given by Fokker-Planck zero diffusion limit, while the particle method gives a different weak solution. Table 1 shows that the convergence rate of the Schrödinger-Poisson solution to the zero diffusion Fokker-Planck equations is of order 1.11 in ϵ in L^1 norm and order 0.69 in L^∞ norm.

Moreover, if we choose another regularization of the δ-function, for instance, the linear kernel approximation below,

$$\psi_0^\epsilon = \sqrt{\delta_b^l(x)}\exp(\frac{iC}{\epsilon}), \quad \text{where } \delta_b^l(x) = \begin{cases} \frac{1}{b}(1 - \left|\frac{x-0.5}{b}\right|), & \left|\frac{x-0.5}{b}\right| \le 1, \\ 0, & \text{otherwise}, \end{cases} \tag{4.2}$$

one can see that from Figure 2, there is no palpable difference between the numerical solutions computed by the cosine kernel approximation and the linear kernel approximation, which gives some evidence that the selection mechanism provided by the semi-classical limit of the Schrödinger-Poisson equations are insensitive to the regularization of the measure-valued initial data.

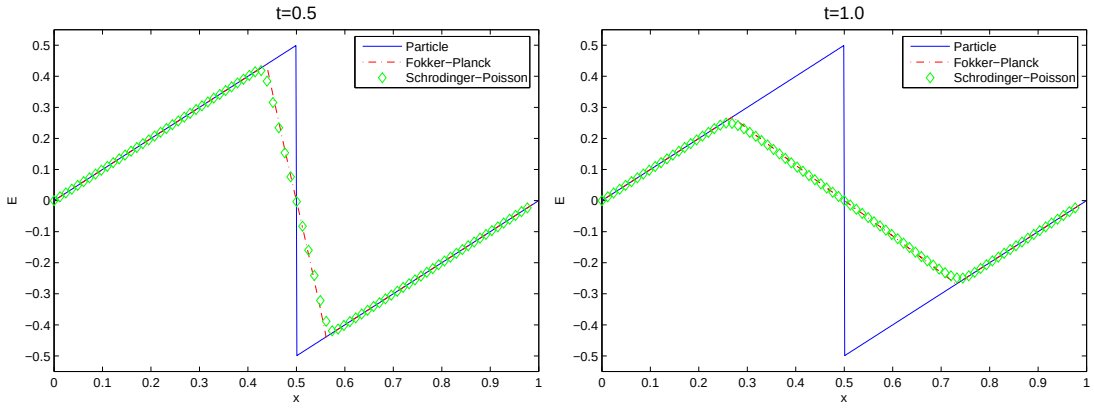

Figure 1: Example 4.1, comparison of the numerical solutions of the electric field E by the Vlasov-Poisson equations and the Fokker-Planck equations, both using the particle method, and the Schrödinger-Poisson equations. Particle number $N = N^* = 8192$, kernel mollifier parameter $\delta = 0.001$, $\Delta t = 0.002$. The viscosity coeffcient for the Fokker-Planck equations is $\eta = 0.001$. In the Schrödinger-Poisson equations, we use the re-scaled Planck constant $\epsilon = 5 \times 10^{-5}$, the constant $C = 1$, $\Delta x = \frac{1}{8192}$, $\Delta t = 0.005$ and δ_b^c given in (4.1). In the figures, "particle" solution refers to the solution of the Vlasov-Poisson equation by the particle method.

ϵ	1×10^{-3}	5×10^{-4}	2.5×10^{-4}
$\|E^\epsilon - E_D\|_\infty$	2.43×10^{-1}	1.63×10^{-1}	9.30×10^{-2}
$\|E^\epsilon - E_D\|_{L^1}$	1.17×10^{-1}	5.96×10^{-2}	2.52×10^{-2}

Table 1: Example 4.1, at $t = 1$, the L^∞ and L^1 errors between the electric field E^ϵ of the Schrödinger-Poisson equations and the electric field E_D of the zero diffusion limit of the Fokker-Planck equations. E_D is approximated by solving the Fokker-Planck equation with the parameters $\eta = 0.0002$, $N = N^* = 16384$ and $\Delta t = 0.001$. E^ϵ is solved by SP2 using $\Delta x = \frac{1}{16384}$, $\Delta t = 0.005$ and δ_b^c given in (4.1).

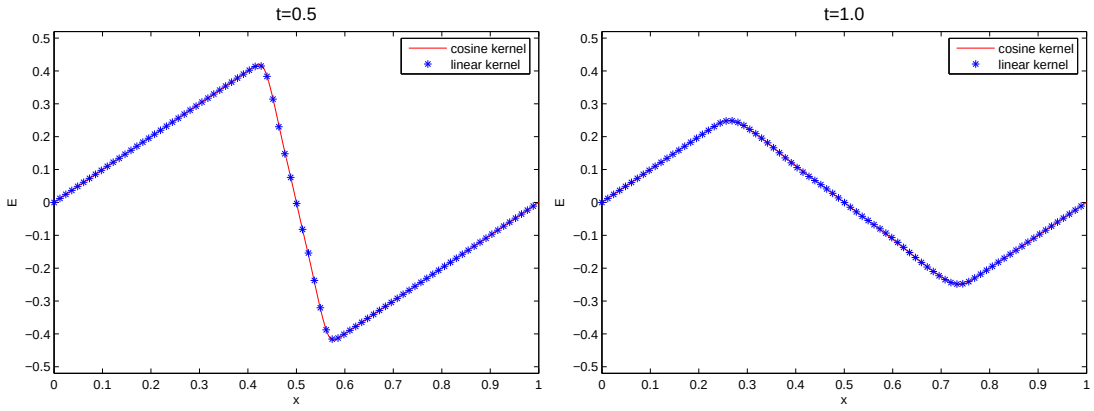

Figure 2: Example 4.1, comparison of the numerical solutions of the electric field E of the Schrödinger-Poisson equations with the cosine kernel approximation δ_b^c in (4.1) and with the linear kernel approximation δ_b^l in (4.2). The re-scaled Planck constant is $\epsilon = 5 \times 10^{-5}$, the constant $C = 1$, $\Delta x = \frac{1}{8192}$ and $\Delta t = 0.005$.

Example 4.2. In this example, we carry out numerical simulations on the three and four particles fission processes. We still use the cosine kernel (4.1) to approximate the delta function. These problems are are similar to the examples used in [14] to show numerical instabilities of the particle method.

- Three particles fission process:
  - The initial condition for the Schrödinger-Poisson equations:

$$\psi_0^\epsilon = \sqrt{\frac{1}{4}\delta_b^c(x-0.25) + \frac{1}{2}\delta_b^c(x-0.5) + \frac{1}{4}\delta_b^c(x-0.75)}\exp(\frac{iC}{\epsilon}), \tag{4.3}$$

  - the initial condition for the Vlasov-Poisson equations and the Fokker-Planck equations:

$$f_0(x,v) = \frac{1}{4}\delta(x-0.25)\delta(v) + \frac{1}{2}\delta(x-0.5)\delta(v) + \frac{1}{4}\delta(x-0.75)\delta(v). \tag{4.4}$$

- Four particles fission process:
  - The initial condition for the Schrödinger-Poisson equations:

$$\psi_0^\epsilon = \sqrt{\frac{1}{4}\sum_{j=1}^{4}\delta_b^c(x-0.2j)}\exp(\frac{iC}{\epsilon}), \tag{4.5}$$

  - the initial condition for the Vlasov-Poisson equations and the Fokker-Planck equations:

$$f_0(x,v) = \frac{1}{4}\sum_{j=1}^{4}\delta(x-0.2j)\delta(v). \tag{4.6}$$

Numerical results are given in Figures 3 and 4, which show that the semiclassical limit solutions agree with the weak solutions given by Fokker-Planck zero diffusion limit. Moreover, with a more refined resolution of the delta-function initial data, we did not observe the numerical instability of the particle method pointed out in [14].

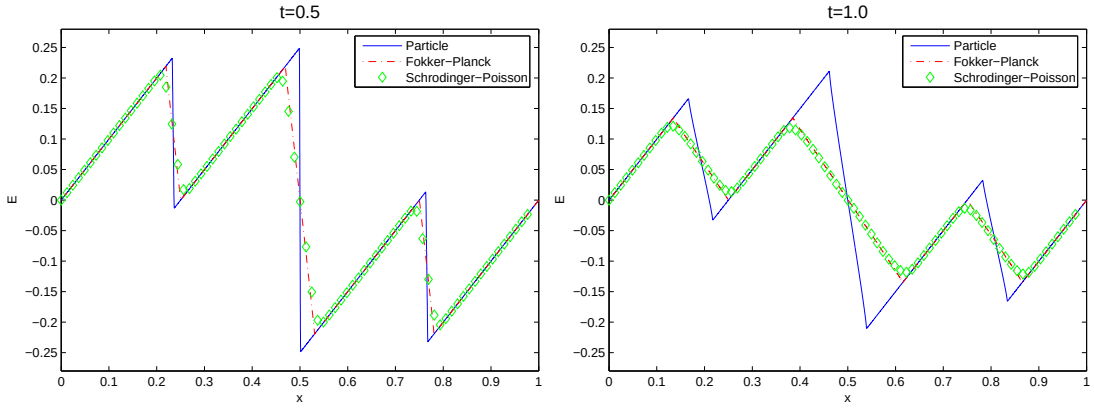

Figure 3: Example 4.2, three particles fission process. Comparison of the numerical solutions of the electric field E by the Vlasov-Poisson equations and the Fokker-Planck equations, both using the particle method, and the Schrödinger-Poisson equations. The parameters and mesh grids are the same as Figure 1 in Example 4.1. In the figures, "particle" solution refers to the solution of the Vlasov-Poisson equation by the particle method.

Example 4.3. In this example, we study the elastic collision case of three particles. We take the initial condition of the Schrödinger-Poisson equations as:

$$\psi_0^\epsilon = \sqrt{\frac{1}{4}\delta_b^c(x-0.25) + \frac{1}{2}\delta_b^c(x-0.5) + \frac{1}{4}\delta_b^c(x-0.75)}\exp\left(-\frac{\cos(2\pi x)}{2\pi\epsilon}\right), \tag{4.7}$$

in which δ_b^c is defined in (4.1). Then the corresponded initial condition of the Vlasov-Poisson equations and the Fokker-Planck equations is given by:

$$f_0(x,v) = \left(\frac{1}{4}\delta(x-0.25) + \frac{1}{2}\delta(x-0.5) + \frac{1}{4}\delta(x-0.75)\right)\delta(v-\sin(2\pi x)). \tag{4.8}$$

Physically, it describes a process where two particles with momentum $1/4$ at $x = 0.25$ and $x = 0.75$ move toward the still one at $x = 0.5$, and after an elastic collision, they exchange momentum and begin to move in the opposite directions. In order to minimize the effect of numerical error in discretizing the delta functions of the particles collision process, we use $\Delta x = \frac{1}{32768}$, $\Delta t = 2\times 10^{-4}$ and the re-scaled Planck constant $\epsilon = 2\times 10^{-5}$ in the computation of the Schrödinger-Poisson equations. The numerical results of the electric field is given in Figure 5, in which convergence of the solution of the Schrödinger-Poisson toward that of the Vlasov-Poission is shown before and after the collision.

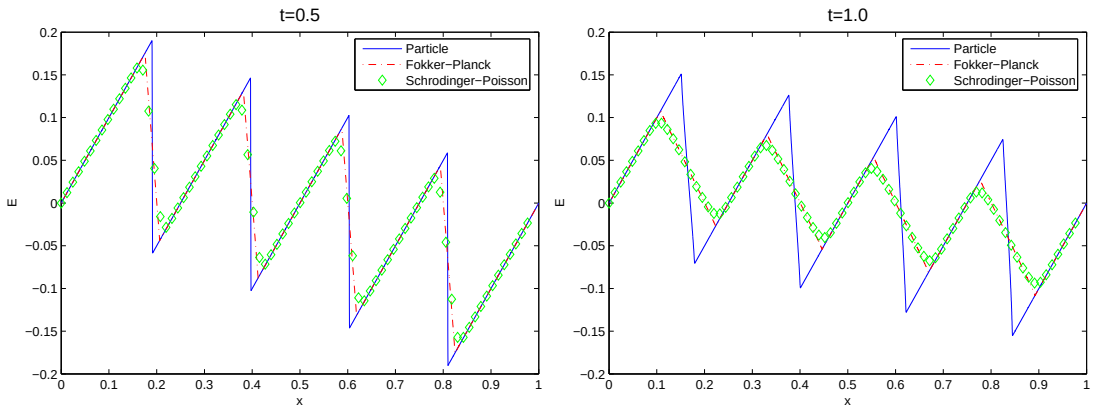

Figure 4: Example 4.2, four particles fission process. Comparison of the numerical solutions of the electric field E by the Vlasov-Poisson equations and the Fokker-Planck equations, both using the particle method, and the Schrödinger-Poisson equations. The parameters and mesh grids are the same as Figure 1 in Example 4.1. In the figures, "particle" solution refers to the solution of the Vlasov-Poisson equation by the particle method.

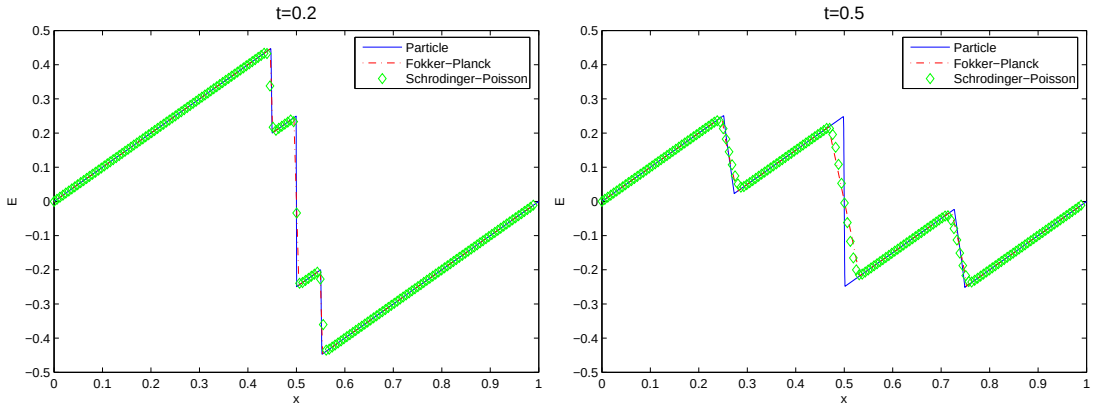

Figure 5: Example 4.3, comparison of the numerical solutions of the electric field E by the Vlasov-Poisson equations and the Fokker-Planck equations, both using the particle method, and the Schrödinger-Poisson equations in the three particles elastic collision process. Left: $t = 0.2$ before the first collision; right: $t = 1.0$ after the collision. Particle number $N = N^* = 8192$, kernel mollifier parameter $\delta = 0.001$, $\Delta t = 0.002$. The viscosity coefficient for the Fokker-Planck equations is $\eta = 0.001$. In the Schrödinger-Poisson equations, we use the re-scaled Planck constant $\epsilon = 2 \times 10^{-5}$. In the figures, "particle" solution refers to the solution of the Vlasov-Poisson equation by the particle method.

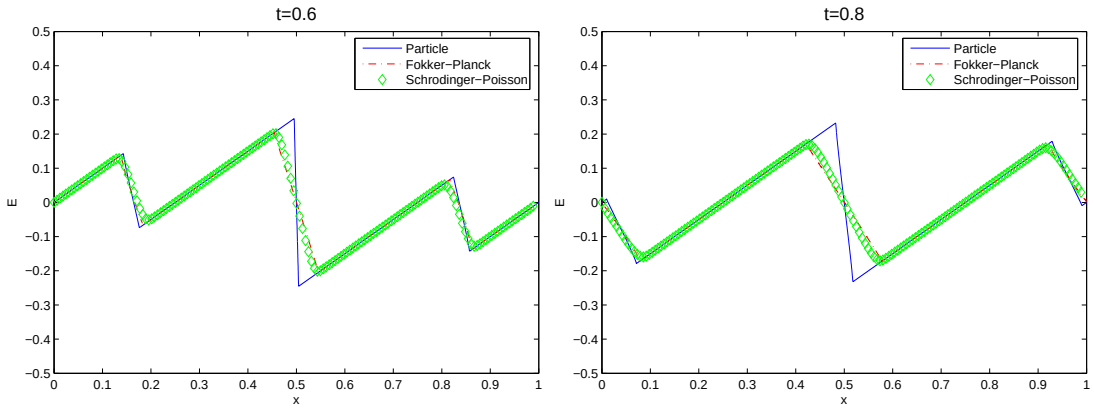

Figure 5: (Continued) Example 4.3, left: $t = 0.5$ before the second collision; right: $t = 1.0$ after the second collision. Note that the two particles collide at $x = 0$ and $x = 1$ for the second time due to the periodic boundary condition.

Example 4.4. Solve the Vlasov-Poisson equations (1.1)-(1.2), the Fokker-Planck equations (1.7)-(1.8), the Schrödinger-Poisson equations (1.10), and the moment equations (3.5) respectively with initial condition $\rho_0(x) = 1$, $u_0(x) = \sin(2\pi x)$, $f_0 = \delta(v - u_0(x))$ and $\psi_0^\epsilon(x) = \exp\left(-\frac{\cos(2\pi x)}{2\pi\epsilon}\right)$.

According to [14], the exact solution of the Vlasov-Poisson equations is given by

$$x(a,t) = a + \sin(2\pi a)\sin(t),\ \ u(x(a,t),t) = \sin(2\pi a)\cos(t), \tag{4.9}$$

$$\rho(x(a,t)) = \left(\frac{dx(a,t)}{da}\right)^{-1}, \tag{4.10}$$

$$E(x(a,t),t) = \sin(2\pi a)\sin(t) - 1 + a + \mathrm{meas}(S^+(x(a,t))) \tag{4.11}$$

where $a \in [0,1]$ is a parameter, $\mathrm{meas}(A)$ means the Lebesgue measure of the set A, and $S^+(x(a,t)) = \{a' : x(a,t) \le x(a',t) \le 1\}$. Note that before the singularity, $S^+(x(a,t)) = \{a' : a \le a' \le 1\}$, and the singularity time is given by

$$t_c = \inf\{t : \frac{dx(a,t)}{da} = 0, 0 \le a \le 1, t \ge 0\}$$

After a simple calculation, one can get $t_c = 0.1598$ in this example.

Figure 6 shows that both the zero smoothing limit of the time reversible particle method and the diffusion limit of the Fokker-Planck equation converge to the same weak solution, the one given by the semi-classical limit of the Schrödinger-Poisson equations. We point out that the solution E of the Schrödinger-Poisson equations is oscillatory, which cannot be seen in the figure but a zoom-in figure shows it which is omitted here. Table 2 shows the convergence rate of the Schrödinger-Poisson is of order 0.82 in ϵ in L^1 norm and order 0.25 in L^∞ norm. The convergence rate in the L^∞ norm is lower because of the singularities (caustics). Since the semiclassical limit is a weak limit, one cannot expect the same strong convergence in the more oscillatory quantities ρ and u.

We get the multi-valued solution for Eq.(1.1)-(1.2) by solving (3.5) with the second order kinetic scheme. The mesh size and time steps are $\Delta x = 1/400$, $\Delta t = \Delta x/5$. The thresholds ϵ_1 and ϵ_2 for the indicator functions θ_1 and θ_2 in (3.8) are $\epsilon_1 = 10^{-4}$, $\epsilon_2 = -10^{-7}$. Note that for the moment system (3.5), the numerical solution ρ_2 often displays spurious peaks ([9]), whereas the multivalued velocities u_1, u_2, and u_3 can usually be well produced. This is because the computation of the multivalued densities involves inverting a matrix of the Vandermonde type, which is ill conditioned near the phase boundaries (i.e. where u_3 or u_1 get close to u_2). Therefore, to compute ρ_2, the strategy proposed by Gosse, Jin and Li (formula (26) in [6]) is used. The numerical results are shown in Fig. 7.

In this example, all methods produce the same weak solutions. In particular, it shows that the moment system gives the weak solution described by the semi-classical limit of the Schrödinger-Poisson equations beyond the caustics.

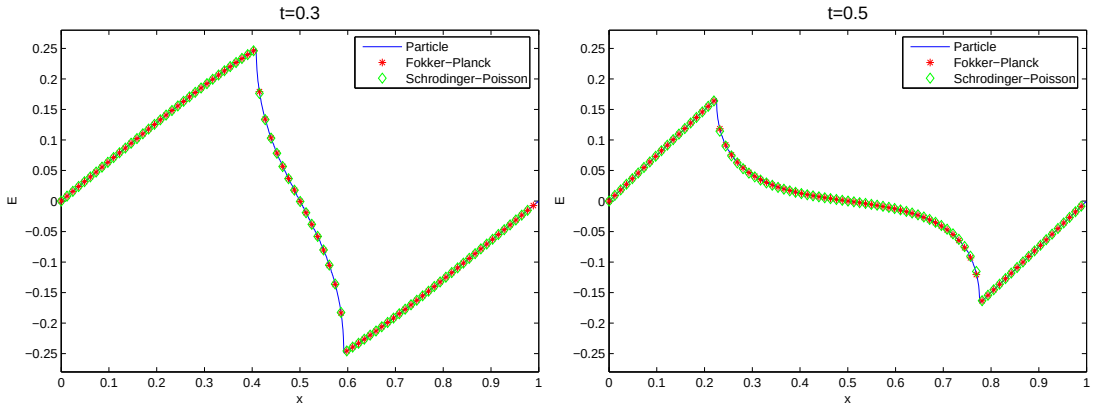

Figure 6: Example 4.4, comparison of the numerical solutions of the electric field E by the Vlasov-Poisson equations and the Fokker-Planck equations, both using the particle method, and by the Schrödinger-Poisson equations. Particle number $N = N^* = 8192$, kernel mollifier parameter $\delta = 0.001$, $\Delta t = 0.002$. The viscosity for the Fokker-Plank equation is $\eta = 0.001$. In the Schrödinger-Poisson, the re-scaled Planck constant is $\epsilon = 5 \times 10^{-5}$, the constant $C = 1$, $\Delta x = \frac{1}{8192}$ and $\Delta t = 0.005$.

ϵ	1×10^{-3}	5×10^{-4}	2.5×10^{-4}
$\|E^\epsilon - E_D\|_\infty$	1.77×10^{-2}	1.43×10^{-2}	1.25×10^{-2}
$\|E^\epsilon - E_D\|_{L^1}$	1.64×10^{-3}	9.24×10^{-4}	5.27×10^{-4}

Table 2: Example 4.4, at $t = 0.5$, the L^∞ and L^1 errors between the electric field E^ϵ of the Schrödinger-Poisson equations and the electric field E_D of the zero diffusion limit of the Fokker-Planck equations. E_D is approximated by solving the Fokker-Planck equation with the parameters $\eta = 0.0002$, $N = N^* = 16384$ and $\Delta t = 0.001$. E^ϵ is solved by SP2 using $\Delta x = \frac{1}{16384}$ and $\Delta t = 0.005$.

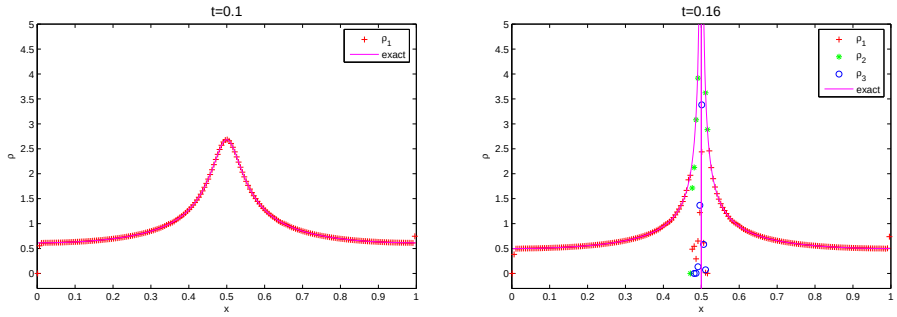

(a) Density

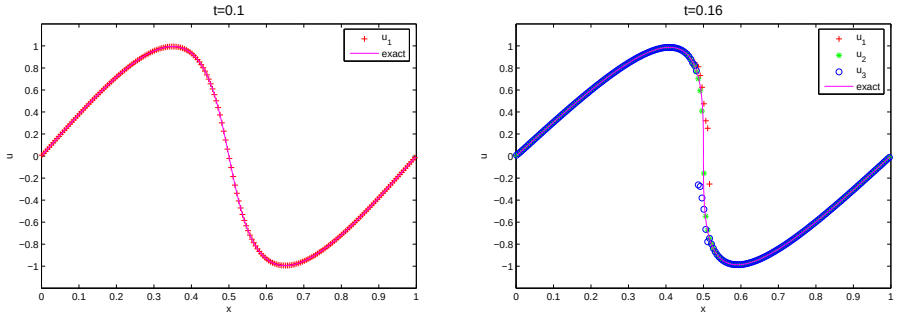

(b) Velocity

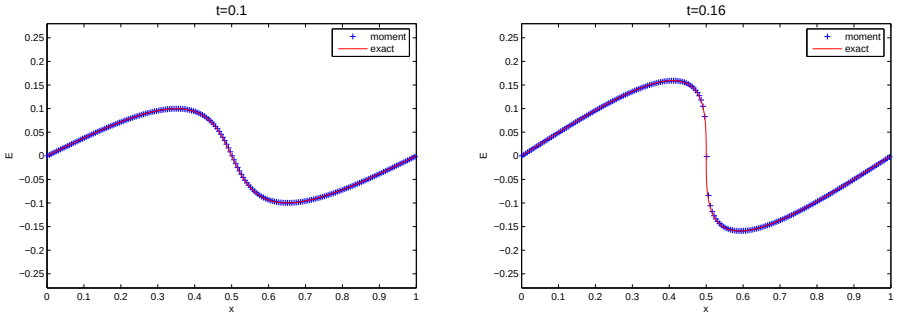

(c) Electric field

Figure 7: Example 4.4, $\Delta x = 1/400$, $\Delta t = \Delta x/5$, $\epsilon_1 = 10^{-4}$, $\epsilon_2 = -10^{-7}$ by using a second order kinetic scheme for the moment system (3.5) with $K = 3$. The figure shows, from top to bottom, the comparison of the density, velocity and the electric field between the moment method and the exact solution (solid line). Left: at $t = 0.1$ before the caustic occurs; right: at the critical time $t = t_c = 0.16$.

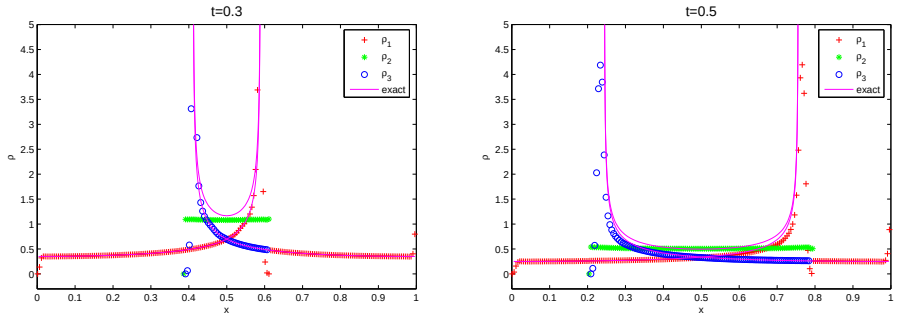

(a) Density

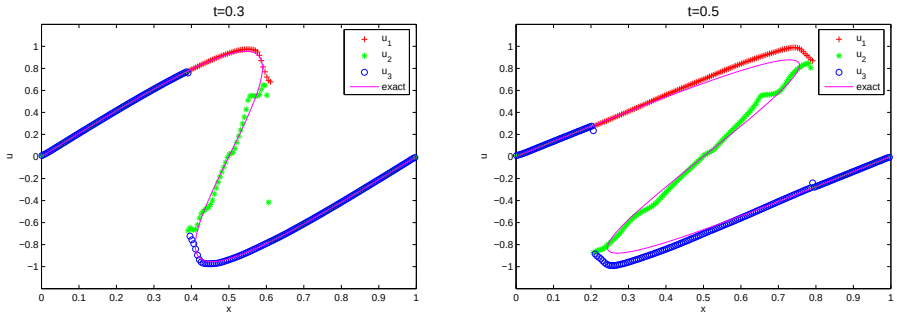

(b) Velocity

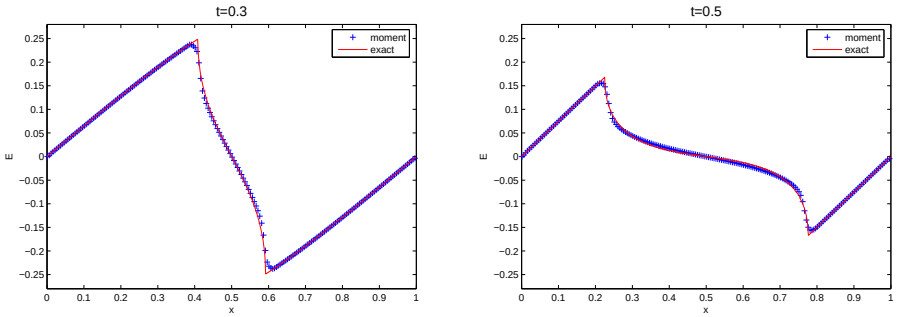

(c) Electric field

Figure 7: (Continued) Example 4.4, left: at $t = 0.3$ after the caustic occurs; right: at $t = 0.5$.

5 Conclusion

Through several numerical examples, we show that the semiclassical limit of the Schrödinger-Poisson equations provides a selection principle for the weak solution of the Vlasov-Poisson equations, which agrees with the diffusion limit of the Fokker-Planck equation. This limit is not sensitive for the discretization of the measure-valued initial data. Furthermore, we show that the semiclassical limit of the Schrödinger-Poission equations gives the weak solution to the Euler-Poission equations governed by a moment system introduced in [9, 10].

In the future we will study these problems in higher space dimensions.

Acknowledgement

We thank Prof. Yuxi Zheng for useful discussion.

References

[1] F. Bouchut, S. Jin and X.T. Li, Numerical Approximations of Pressureless and Isothermal Gas Dynamics, SIAM J. Num. Anal. 41 (2003), 135-158.

[2] W.Z. Bao, S. Jin and P.A. Markowich, On time-spliting spectral approximations for the Schrödinger equation in the semiclassical regime. J. Comp. Phys. 175 (2002), 487-524.

[3] W.Z. Bao, S. Jin and P.A. Markowich, Numerical Study of Time-Splitting Spectral Discretizations of Nonlinear Schrodinger Equations in the Semi-clasical Regimes. SIAM J. Sci. Comp. 25 (2003), 27-64 (elctronic).

[4] G.H. Cottet and P.A. Raviart, Particle methods for the 1D Vlasov-Poisson equations, SIAM J. Num. Anal. 21 (1984) 52-76.

[5] B. Engquist, A.K. Tornberg and R. Tsai, Discretization of Dirac Delta Functions in Level Set Methods. J. Comput. Phys. 207 (2005), no. 1, 28–51.

[6] L. Gosse, S. Jin and X.T. Li, On Two Moment Systems for Computing Multiphase Semiclassical Limits of the Schrödinger Equation. Math. Model Methods Appl. Sci. 13, No. 12 (2003), 1689-1723.

[7] L. Gosse and N.J. Mauser, Multiphase semiclassical approximation of an electron in a one-dimensional crystalline lattice C III. From ab initio models to WKB for Schrödinger-Poisson, J. Comp. Phys. 211 (2006), 326-346.

[8] P. Gerard, P.A. Markowich, N.J. Mauser, F. Poupaud, Homogenization Limits and Wigner Transforms. Comm. Pure Appl. Math. 50 (4) (1997), 323-379.

[9] S. Jin and X.T. Li, Multi-phase computations of the semiclassical limit of the Schrödinger equation and related problems: Whitham vs Wigner, Physica D, 182 (2003), 46-85.

[10] X.T. Li, J.G. Wohlbier, S. Jin and J.H. Booske, An Eulerian method for computing multi-valued solutions of the Euler-Poisson equations and applications to wave breaking in klystrons, Phys. Rev. E. 70 (2004), 016502.

[11] P.-L. Lions and T. Paul, Sur les measure de Wigner. Rev. Mat. Iberoamericana 9 (1993), no. 3, 553 - 618.

[12] H. Liu and Z.M. Wang, A field space-based level set method for computing multi-valued solutions to 1D Euler-Poisson equations, J. Comp. Phys., to appear.

[13] P.A. Markowich and N.J. Mauser, The classical limit of a self-consistent quantum-Vlasov equation in 3D. Math. Models and Methods in Applied Sciences, Vol. 3, No. 1 (1993), 109-124.

[14] A.J. Majda, G. Majda and Y.X. Zheng, Concentrations in the one-dimensional Vlasov-Poisson equations: Temporal development and non-unique weak solutions in the single component case. Physica D, 74(1994), 268-300.

[15] C. Sparber, P.A. Markowich and N.J. Mauser, Wigner functions vs. WKB methods in multivalued geometrical optics, Asympt. Anal. 33 (2003), 153 - 187.

[16] E. Wigner, On the quantum correction for thermodynamic equilibrium. Phys. Rev. 40 (1932), 749-759.

[17] P. Zhang, Y.X. Zheng and N.J. Mauser, The limit from the Schrödinger-Poisson to the Vlasov-Poisson equations with general data in one dimension. Comm. on Pure and Applied Mathematics, Vol.LV (2002), 0582-0632.

[18] Y.X. Zheng and A. Majda, Existence of global weak solutions to one-component Vlasov-Poisson and Fokker-Planck-Poisson systems in one space dimension with measures as initial data. Comm. on Pure and Applied Math. Vol. XLVII (1994), 1365-1401.